

## **A Robust Image Denoising Using Modified Discrete Curvelet Transform with Ridgelet Transforms**



**Sanku Koteswaramma**  
M.Tech in DECS,  
Department of ECE

Vignan's Nirula Institute of Technology & Science for Women, Guntur, Andrapradesh, India.



**Koganti Nalini**  
Assistant Professor  
Department of ECE

Vignan's Nirula Institute of Technology & Science for Women, Guntur, Andrapradesh, India.

### **ABSTRACT**

In any application image denoising is a challenging task because noise removal will increase the digital quality of an image and will improve the perceptual visual quality. In spite of the great success of many denoising algorithms, they tend to smooth the fine scale image textures when removing noise, degrading the image visual quality. To address this problem, in this paper we propose Modified Discrete Curvelet Transform (M-DCVT). Simulation results show that the proposed method has given the better performance when compared to the existing algorithms in terms of peak signal to noise ratio (PSNR) and mean square error (MSE).

### **I. INTRODUCTION**

Images captured from both digital cameras and conventional film cameras will be affected with the noise from a variety of sources. These noise elements will create some serious issues for further processing of images in practical applications such as computer vision, artistic work or marketing and also in many fields. There are many types of noises like salt and pepper, Gaussian, speckle and poisson. In salt and pepper noise (sparse light and dark disturbances), pixels in the captured image are very different in intensity from their neighbouring pixels; the defining characteristic is that the intensity value of a noisy picture element bears no relation to the color of neighbouring pixels. Generally, this type of noise will

only affect a small number of pixels in an image. When we viewed an image which is affected with salt and pepper noise, the image contains black and white dots, hence it is termed as salt and pepper noise. In Gaussian noise, noisy pixel value will be a small change of original value of a pixel. A histogram, a discrete plot of the amount of the distortion of intensity values against the frequency with which it occurs, it shows a normal distribution of noise. While other distributions are possible, the Gaussian (normal) distribution is usually a good model, due to the central limit theorem that says that the sum of different noises tends to approach a Gaussian distribution. In selecting a noise reduction algorithm, one must consider several factors:

- A digital camera must apply noise reduction in a fraction of a second using a tiny on board CPU, while a desktop computer has much more power and time
- whether sacrificing some real detail information is acceptable if it allows more distortion or noise to be removed (how aggressively to decide whether the random variations in the image are noisy or not)

In real-world photographs, maximum variations in brightness ("luminance detail") will be consisted by the highest spatial frequency, rather than the random variations in hue ("chroma detail"). Since most of noise reducing techniques should attempt to remove

noise without destroying of real detail from the captured photograph. In addition, most people find luminance noise in images less objectionable than chroma noise; the colored blobs are considered "digital-looking" and artificial, compared to the mealy appearance of luminance noise that some compare to film grain. For these two reasons, most of digital image noise reduction algorithms split the image content into chroma and luminance components. One solution to eliminate noise is by convolving the original image with a mask that represents a low-pass filter or smoothing operation. For example, the Gaussian mask incorporates the elements determined by a Gaussian function. This operation brings the value of each pixel into closer harmony with the values of its neighbors. In general, a smoothing filter sets each pixel to the mean value, or a weighted mean, of itself and its nearby neighbors; the Gaussian filter is just one possible set of weights. However, spatial filtering approaches like mean filtering or average filtering, Savitzky filtering, Median filtering, bilateral filter and Wiener filters had been suffered with losing edges information. All the filters that have been mentioned above were good at denoise of images but they will provide only low frequency content of an image it doesn't preserve the high frequency information. In order to overcome this issue Non Local mean approach has been introduced. More recently, noise reduction techniques based on the "NON-LOCAL MEANS (NLM) had developed to improve the performance of denoising mechanism [1][4][5][9]. It is a data-driven diffusion mechanism that was introduced by Buades *et al.* in [1]. It has been proved that it's a simple and powerful method for digital image denoising. In this, a given pixel is denoised using a weighted average of other pixels in the (noisy) image. In particular, given a noisy image  $n_i$ , and the denoised image  $\hat{d} = \hat{d}_i$  at pixel  $i$  is computed by using the formula

$$\hat{d}_i = \frac{\sum_j w_{ij} n_j}{\sum_j w_{ij}} \quad (1)$$

Where  $w_{ij}$  is some weight assigned to pixel  $i$  and  $j$ .

The sum in (1) is ideally performed to whole image to denoise the noisy image. NLM at large noise levels

will not give accurate results because the computation of weights of pixels will be different for some neighbourhood pixels which looks like same. Most of the standard algorithm used to denoise the noisy image and perform the individual filtering process. Denoise generally reduce the noise level but the image is either blurred or over smoothed due to losses like edges or lines. In the recent years there has been a fair amount of research on center pixel weight (CPW) for image denoising [3], because CPW provides an appropriate basis for separating noisy signal from the image signal. Optimized CPW is good at energy compaction, the small coefficient are more likely due to noise and large coefficient due to important signal feature [8]. These small coefficients can be thresholded without affecting the significant features of the image. However, all the above mentioned techniques were not suitable for texture enhanced image denoising and will not preserve the fine details of image. In order to overcome the existing systems drawbacks, here in this we propose a texture enhanced image denoising algorithm from the given noisy image  $y$ , we estimate the gradient histogram of original image  $x$ . Taking this estimated histogram, denoted by  $h$ , as a reference, we search an estimate of  $x$  such that its gradient histogram is close to  $h_r$ . As shown in Fig. 1, the proposed GHP based denoising method can well enhance the image texture regions, which are often over-smoothed by other denoising methods. The major contributions of this paper are summarized as follows:

- (1) A novel texture enhanced image denoising framework is proposed, which preserves the gradient histogram of the original image. The existing image priors can be easily incorporated into the proposed framework to improve the quality of denoised images.
- (2) Using histogram specification, a gradient histogram preservation algorithm is developed to ensure that the gradient histogram of denoised image is close to the reference histogram, resulting in a simple yet effective GHP based denoising algorithm.
- (3) By incorporating the hyper-Laplacian and nonnegative constraints, a regularized deconvolution model and an iterative deconvolution algorithm.

In this letter, we discuss the texture enhancement (TE) problem with GHP and IHS specification algorithm. The rest of this thesis has been organized as: Section II existing techniques such as Savitzky-golay, median, bilateral, wavelet filters, and NLM; Section III discusses the new solution of the TE problem; Section IV shows experimental comparisons for various techniques with the new solution; and Section V concludes the thesis.

## II. EXISTING TECHNIQUES

In this section we discussed various spatial filters and their performance when a noisy input will be given to them. Here in this section we had explained about each filter in detail. Firstly, *Savitzky-Golay (SG) filter*: it is a simplified method and uses least squares technique for calculating differentiation and smoothing of data. Its computational speed will be improved when compared least-squares techniques. The major drawback of this filter is: Some of first and last data point cannot smoothen out by the original Savitzky-Golay method. Assuming that, filter length or frame size (in S-G filter number of data sample read into the state vector at a time)  $N$  is odd,  $N=2M+1$  and  $N= d+1$ , where  $d$ = polynomial order or polynomial degree. Second, *Median filter*: This is a nonlinear digital spatial filtering technique, often used to removal of noise from digital images. Median filtering has been widely used in most of the digital image processing applications. The main idea of the median filter is to run through the image entry by pixel, replacing each pixel with the median value of neighboring pixels. The pattern of neighbors is called the "window", which slides, pixel by pixel, over the entire image. Third, *Bilateral filter*: The bilateral filter is a nonlinear filter which does the spatial averaging without smoothing edges information. Because of this feature it has been shown that it's an effective image denoising algorithm. Bilateral filter is presented by Tomasi and Manduchi in 1998. The concept of the bilateral filter was also presented in [8] as the SUSAN filter and in [3] as the neighborhood filter. It is mentionable that the Beltrami flow algorithm is considered as the theoretical origin of the bilateral filter [4] [5] [6], which produce a

spectrum of image enhancing algorithms ranging from the linear diffusion to the non-linear flows. The bilateral filter takes a weighted sum of the pixels in a local neighborhood; the weights depend on both the spatial distance and the intensity length. In this way, edges are preserved well while noise is eliminated out. Next, *Wavelet filtering*: Signal denoising using the DWT consists of the three successive procedures, namely, signal decomposition, thresholding of the DWT coefficients, and signal reconstruction. Firstly, we carry out the wavelet analysis of a noisy signal up to a chosen level  $N$ . Secondly, we perform thresholding of the detail coefficients from level 1 to  $N$ . Lastly, we synthesize the signal using the altered detail coefficients from level 1 to  $N$  and approximation coefficients of level  $N$ . However, it is generally impossible to remove all the noise without corrupting the signal. As for thresholding, we can settle either a level-dependent threshold vector of length  $N$  or a global threshold of a constant value for all levels. *Classical Non Local Means*: It is a data-driven diffusion mechanism that was introduced by Buades *et al.* in [1]. It has been proved that it's a simple and powerful method for digital image denoising. In this, a given pixel is denoised using a weighted average of other pixels in the (noisy) image. In particular, given a noisy image  $n_i$ , and the denoised image  $\hat{d} = \hat{d}_i$  at pixel  $i$  is computed by using the formula

$$\hat{d}_i = \frac{\sum_j w_{ij} n_j}{\sum_j w_{ij}} \quad (1)$$

Where  $w_{ij}$  is some weight assigned to pixel  $i$  and  $j$ . The sum in (1) is ideally performed to whole image to denoise the noisy image. NLM at large noise levels will not give accurate results because the computation of weights of pixels will be different for some neighbourhood pixels which looks like same.

$$w_{i,j} = \exp\left(\sum_{k \in P} G_\beta \left(\frac{(n_{i+k} - n_{j+k})^2}{2h}\right)\right) \quad (2)$$

In this each weight is computed by similarity quantification between two local patches around noisy pixels  $n_i$  and  $n_j$  as shown in eq. (2). Here,  $G_\beta$  is a

Gaussian weakly smooth kernel [1] and  $P$  denotes the local patch, typically a square centered at the pixel and  $h$  is a temperature parameter controlling the behavior of the weight function.

Another popular approach to image denoising is the variational method, where energy functional is minimized to search the desired estimation of  $x$  from its noisy observation  $y$ . The energy functional usually involves two terms: a data fidelity term which depends on the image degeneration process and a regularization term which models the prior of clean natural images [13], [16] and [17]. The statistical modeling of natural image priors is crucial to the success of image denoising. Motivated by the fact that natural image gradients and wavelet transform coefficients have a heavy-tailed distribution, sparsity priors are widely used in image denoising [10]–[12].

The well-known total variation minimization methods actually assume Laplacian distribution of image gradients [13]. The sparse Laplacian distribution is also used to model the high pass filter responses and wavelet/curvelet transforms coefficients [14], [15]. By representing image patches as a sparse linear combination of the atoms in an over-complete redundant dictionary, which can be analytically designed or learned from natural images, sparse coding has proved to be very effective in image denoising via  $l_0$ -norm or  $l_1$ -norm minimization [16], [17]. Another popular prior is the nonlocal self-similarity (NSS) prior that is, in natural images there are often many similar patches (i.e., nonlocal neighbors) to a given patch, which may be spatially far from it. The connection between NSS and the sparsity prior is discussed in [18], [19]. The joint use of sparsity prior and NSS prior has led to state-of-the-art image denoising results [19]–[14]. In spite of the great success of many denoising algorithms, however, they often fail to preserve the image fine scale texture structures, degrading much the image visual quality (please refer to Fig. 1 for example). With the rapid development of digital imaging technology, now the acquired images

can contain tens of megapixels. On one hand, more fine scale texture features of the scene will be captured; on the other hand, the captured high definition image is more prone to noise because the smaller size of each pixel makes the exposure less sufficient. Unfortunately, suppressing noise and preserving textures are difficult to achieve simultaneously, and this has been one of the most challenging problems in natural image denoising. Unlike large scale edges, the fine scale textures are much more complex and are hard to characterize by using a sparse model. Texture regions in an image are homogeneous and are composed of similar local patterns, which can be characterized by using local descriptors or textons. Cognitive studies have revealed that the first-order statistics, e.g., histograms, are the most significant descriptors for texture discrimination. Considering these facts, histogram of local features has been widely used in texture analysis [24]–[26].

Meanwhile, image gradients are crucial to the perception and analysis of natural images. All these motivate us to use the histogram of image gradient to design new image denoising models. With the above considerations, a novel gradient histogram preservation (GHP) method for texture enhanced image denoising has been used.

The noisy observation  $y$  of an unknown clean image  $x$  is usually modeled as

$$y = x + v \quad (1)$$

where  $v$  is the additive white Gaussian noise (AWGN) with zero mean and standard deviation  $\sigma$ . The goal of image de-noising is to estimate the desired image  $x$  from  $y$ . One popular approach to image denoising is the variational method, in which the denoised image is obtained by

$$\hat{x} = \arg \min_x \left\{ \frac{1}{2\sigma^2} \|y - x\|^2 + \lambda \cdot R(x) \right\} \quad (2)$$

where  $R(x)$  denotes some regularization term and  $\lambda$  is a positive constant. The specific form of  $R(x)$  depends on the employed image priors. One common problem of image denoising methods is that the image fine scale details such as texture structures will be over-smoothed. An over-smoothed image will have much



weaker gradients than the original image. Intuitively, a good estimation of  $x$  without smoothing too much the textures should have a similar gradient distribution to that of  $x$ . With this motivation, we propose gradient histogram preservation (GHP) model for texture enhanced image denoising, whose framework is illustrated in Fig. 1.

Suppose that we have an estimation of the gradient histogram of  $x$ , denote by  $h_r$ . In order to make the gradient histogram of denoised image  $\hat{x}$  nearly the same as the reference histogram  $h_r$ , we propose the following GHP based image denoising model:

$$\hat{x} = \arg \min_x \left\{ \frac{1}{2\sigma^2} \|y - x\|^2 + \lambda R(x) + \mu \|F(\nabla x) - \nabla x\|^2 \right\} \quad (3)$$

Where  $F$  denotes an odd function which is monotonically non-descending,  $h_F$  denotes the histogram of the transformed gradient image  $|F(\nabla x)|$ ,  $\nabla$  denotes the gradient operator, and  $\mu$  is a positive constant. The proposed GHP algorithm adopts the alternating optimization strategy. Given  $F$ , we can fix  $\nabla x_0 = F(\nabla x)$ , and update  $x$ . Given  $x$ , we can update  $F$  by the histogram specification based shrinkage operator. Thus, by introducing  $F$ , we can easily incorporate the gradient histogram constraint with any existing image regularizer  $R(x)$ .

Another issue in the GHP model is how to find the reference histogram of  $h_r$  unknown image  $x$ . In practice, we need to estimate  $h_r$  based on the noisy observation  $y$ . In Section algorithm1, we will propose a regularized deconvolution model and an associated iterative deconvolution algorithm to estimate  $h_r$  from the given noisy image. Once the reference histogram  $h_r$  is obtained, the GHP algorithm is then applied for texture enhanced image denoising.

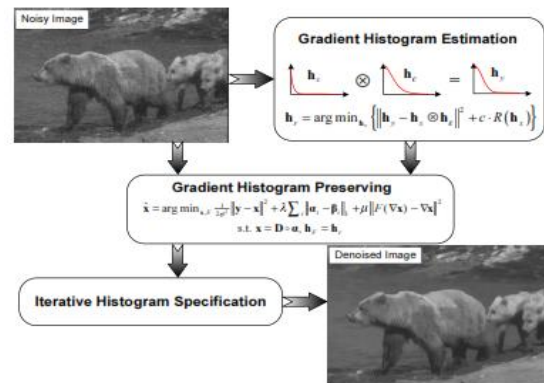


Fig1. framework flow chart for texture enhanced image denoising

The denoising method is a patch based method. Let  $x_i = R_i x$  be a patch extracted at position  $i, i = 1, 2, \dots, N$ , where  $R_i$  is the patch extraction operator and  $N$  is the number of pixels in the image. Given a dictionary  $D$ , we sparsely encode the patch  $x_i$  over  $D$ , resulting in a sparse coding vector  $\alpha_i$ . Once the coding vectors of all image patches are obtained, the whole image  $x$  can be reconstructed by [16]:

$$x = D \circ \alpha \triangleq \left( \sum_{i=1}^N R_i^T R_i \right)^{-1} \sum_{i=1}^N R_i^T D \alpha_i \quad (4)$$

where  $\alpha$  is the concatenation of all  $\alpha_i$ .

Good priors of natural images are crucial to the success of an image denoising algorithm. A proper integration of different priors could further improve the denoising performance. For example, the methods in [21]-[23] integrate image local sparsity prior with nonlocal NSS prior, and they have shown promising denoising results. In the proposed GHP model, we adopt the following sparse nonlocal regularization term proposed in the non locally centralized sparse representation (NCSR) model [14]:

$$R(x) = \sum_i \|\alpha_i - \beta_i\|_1, \text{ s.t. } x = D \circ \alpha \quad (5)$$

where  $\beta_i$  is defined as the weighted average of  $\alpha_i^q$ :

$$\beta_i = \sum_q w_i^q \alpha_i^q \quad (6)$$

and  $\alpha_i^q$  is the coding vector of the  $q_{th}$  nearest patch (denoted by  $x_i^q$ ) to  $x_i$ . The weight is defined as  $w_i^q = \frac{1}{w} \exp\left(-\frac{1}{h} \|\hat{x}_i - \hat{x}_i^q\|^2\right)$  (and  $\hat{x}_i$  and  $\hat{x}_i^q$  denote the current estimates of  $\hat{x}_i$  and  $\hat{x}_i^q$ , respectively), where  $h$  is a pre defined constant and  $W$  is the normalization

factor. More detailed explanations on NCSR can be found in [14]. By incorporating the above  $R(x)$  into Eq. (3), the GHP model can be formulated as:  $\hat{x} = \arg \min_{x,F} \left\{ \frac{1}{2\sigma^2} \|y - x\|^2 + \lambda \sum_i \|\alpha_i - \beta_i\|_1 + \mu \|F(\nabla x) - \nabla x\|^2 \right\}$  s.t.  $x = D \circ \alpha, h_F = h_r$  (7)

From the GHP model with sparse nonlocal regularization in Eq. (7), one can see that if the histogram regularization parameter  $\mu$  is high, the function  $F(\nabla x)$  will be close to  $\nabla x$ . Since the histogram  $h_F$  is required to be the same as  $h_r$ , the histogram of  $\nabla x$  will be similar to  $h_r$ , leading to the desired gradient histogram preserved image denoising. In the next subsection, we will see that there is an efficient iterative histogram specification algorithm to solve the model in above Eq. (7).

**Iterative Histogram Specification Algorithm**

The GHP model in Eq. (7) can be solved by using the variable splitting (VS) method, which has been widely adopted in image restoration [40]–[42]. By introducing a variable  $g = F(\nabla x)$ , we adopt an alternating minimization strategy to update  $x$  and  $g$  alternatively. Given  $g = F(\nabla x)$ , we update  $x$  (i.e.,  $\alpha$ ) by solving the following sub-problem:  $\min_x \left\{ \frac{1}{2\sigma^2} \|y - x\|^2 + \lambda \sum_i \|\alpha_i - \beta_i\|_1 + \mu \|F(\nabla x) - \nabla x\|^2 \right\}$  s.t.  $x = D \circ \alpha$  (8)

We use the method in [23] to construct the dictionary  $D$  adaptively. Based on the current estimation of image  $x$ , we cluster its patches into  $K$  clusters, and for each cluster, a PCA dictionary is learned. Then for each given patch, we first check which cluster it belongs to, and then use the PCA dictionary of the cluster as  $D$ . Although in Eq. (8) the  $l_1$  - norm regularization is imposed on  $\|\alpha_i - \beta_i\|_1$  rather than  $\|\alpha_i\|_1$ , by introducing a new variable  $\vartheta_i = \alpha_i - \beta_i$ , we can use the iterative shrinkage/thresholding method [33] to update  $\vartheta_i$  and then update  $\alpha_i = \vartheta_i + \beta_i$ . This strategy is also used in [23] to solve the problem with this

regularization term, and thus here we omit the detailed deduction process.

To get the solution to the sub-problem in Eq. (8), we first use a gradient descent method to update  $x$ :  $x^{(k+1/2)} = x^{(k)} + \delta \left( \frac{1}{2\sigma^2} (y - x^{(k)}) + \mu \nabla^T (g - \nabla x^{(k)}) \right)$

Where  $\delta$  is a pre-specified constant. Then, the coding coefficients  $\alpha_i$  are updated by

$$\alpha_i^{(k+1/2)} = D^T R_i x^{(k+1/2)}$$

By using Eq. (6) to obtain  $\beta_i$ , we further update  $\alpha_i$  by

$$\alpha_i^{(k+1)} = S_{y/d}(\alpha_i^{(k+1/2)} - \beta_i) + \beta_i$$

Where  $S_{y/d}$  is the soft-thresholding operator, and  $d$  is a constant to guarantee the convexity of the surrogate function [33]. Finally, we update  $x^{(k+1)}$  by

$$x^{(k+1)} = D \circ \alpha^{(k+1)} \triangleq \left( \sum_{i=1}^N R_i^T R_i \right)^{-1} \left( \sum_{i=1}^N R_i^T D \alpha_i^{(k+1)} \right)$$

Once the estimate of image  $x$  is given, we can update  $F$  by solving the following sub-problem:

$$\min_{g,F} \|g - \nabla x\|^2 \text{ s.t. } h_F = h_r, g = F(\nabla x).$$

Considering the equality constraint  $g = F(\nabla x)$ , we can substitute  $g$  in  $\|g - \nabla x\|^2$  with  $F(\nabla x)$ , and the sub-problem becomes  $\min_g \|F\nabla x - \nabla x\|^2$  s.t.  $h_F = h_r$ . To

solve this sub-problem, by introducing  $d_0 = |\nabla x|$ , the standard histogram specification operator [34] can be used to obtain the only feasible monotonic non-parametric transform  $T$  which makes the histogram of  $T(d_0)$  the same as  $h_r$ . Note that  $(x - y)^2 \leq ((-x) - y)^2$  if the signs of  $x$  and  $y$  are the same. Since  $F\nabla x = T(|\nabla x|)$ , to minimizing the squared error  $\|F\nabla x - \nabla x\|^2$ , we should require that sign of  $\hat{F}(\nabla x)$  is the same as that of  $\nabla x$ . Thus, we define  $\hat{F}(\nabla x)$  as

$$\hat{F}(\nabla x) = \text{sgn}(\nabla x) T(|\nabla x|)$$

Given  $\hat{F}(\nabla x)$ , we then let  $g = \hat{F}(\nabla x)$ .

The proposed iterative histogram specification (IHS) based GHP algorithm is summarized in **Algorithm 1**. It should be noted that, for any gradient based image denoising model, we can easily adapt the proposed

GHP to it by simply modifying the gradient term and adding an extra histogram specification operation.

**Algorithm 1: Iterative Histogram Specification (IHS) for GHP**

1. Initialize  $k = 0, x^{(k)} = y$
2. Iterate on  $k = 0, 1, \dots, J$
3. Update  $g$  as  $g = F(\nabla x)$
4. Update  $x$ :
 
$$x^{(k+1/2)} = x^{(k)} + \delta \left( \frac{1}{2\sigma^2} (y - x^{(k)}) + \mu \nabla^T (g - \nabla x^{(k)}) \right)$$
5. Update the coding coefficients of each patch:
 
$$\alpha_i^{(k+1/2)} = D^T R_i x^{(k+1/2)}$$
6. Update the non-local mean of coding vector  $\alpha_i \beta_i = \sum_q w_i^q \alpha_i^q$
7. Update  $\alpha$ :
 
$$\alpha_i^{(k+1)} = S_{y/d} (\alpha_i^{(k+1/2)} - \beta_i) + \beta_i$$
8. Update  $x$ :
 
$$x^{(k+1)} = D \circ \alpha^{(k+1)}$$
9.  $F(\nabla x) = \text{sgn}(\nabla x) T(|\nabla x|)$
10.  $k \leftarrow k + 1$
11.  $x = x^{(k)} + \delta (\mu \nabla^T (g - \nabla x^{(k)}))$

**III. PROPOSED FRAME WORK**

The discrete curvelet transform of a continuous function  $f(x_1, x_2)$  makes use of a dyadic sequence of scales, and a bank of filters  $(P_0 f, \Delta_1 f, \Delta_2 f, \dots)$  with the property that the pass band filter  $\Delta_s$  is concentrated near the frequencies  $[2^s, 2^{2s+2}]$ . In wavelet theory, one uses decomposition into dyadic subbands  $[2^s, 2^{2s+2}]$ . In contrast, the subbands used in the discrete curvelet transform of continuous functions have the non-standard form  $[2^s, 2^{2s+2}]$ . This is non-standard feature of the discrete curvelet transform well worth remembering.

The curvelet decomposition is the sequence of the following steps:

- **Subband Decomposition:** The object  $f$  is decomposed into subbands

$$f \mapsto (P_0 f, \Delta_1 f, \Delta_2 f, \dots)$$

- **Smooth Partitioning:** Each subband is smoothly windowed into “squares” of an appropriate scale (of side length  $\sim 2^{-s}$ )

$$\Delta_s f \mapsto (w_Q \Delta_s f)_{Q \in Q_s}$$

- **Renormalization:** Each resulting square is renormalized to unit scale

$$g_Q = (T_Q)^{-1} (w_Q \Delta_s f), Q \in Q_s$$

- **Ridgelet Analysis:** Each square is analyzed via the discrete ridgelet transform.

In this definition, the two dyadic subbands  $[2^s, 2^{2s+1}]$  and  $[2^{2s+1}, 2^{2s+2}]$  are merged before applying the ridgelet transform.

**Algorithm 2**

We now present a sketch of the discrete curvelet transform algorithm:

- 1) Apply the à trous algorithm with scales
- 2) Set  $B = B_{min}$
- 3) For  $j = 1, 2, 3, \dots, J$  do
  - a) Partition the subband  $w_j$  with a block size  $B_j$  and apply the digital ridgelet transform to each block
  - b) If  $j \text{ modulo } 2 = 1$  then  $B_{j+1} = 2B_j$
  - c) else  $B_{j+1} = B_j$

**IV. SIMULATION RESULTS**

Experimental results have been done in MATLAB 2014a version with 4GB RAM and i3 processor. To verify the performance of the GHP based image denoising method and Modified discrete curvelet transform (M-DCVT), we apply it to natural images with various texture structures and also applied to satellite images. All the test images are gray-scale images with gray level ranging from 0 to 255. We first discuss the parameter setting in our GHP algorithm, and then compare the performance of global based GHP and its region based variants. Finally, experiments are conducted to validate its performance in comparison with the state-of-the-art denoising algorithms.

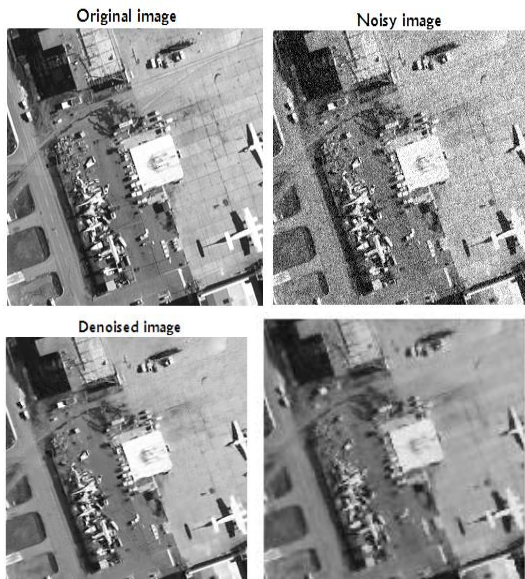


Fig2. (a) Original image, (b) Noisy image and (c) GHP algorithm and (d) proposed MDCVT

There are 4 parameters in our GHP algorithm and 4 parameters in the reference histogram estimation algorithm. All these parameters are fixed in our experiments. Then after we compared the denoised image of proposed M-DCVT with existing GHP algorithm.

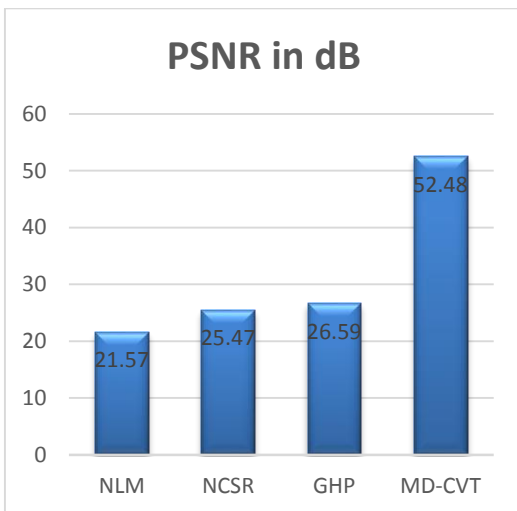


Fig3. Variation of PSNR with sigma value

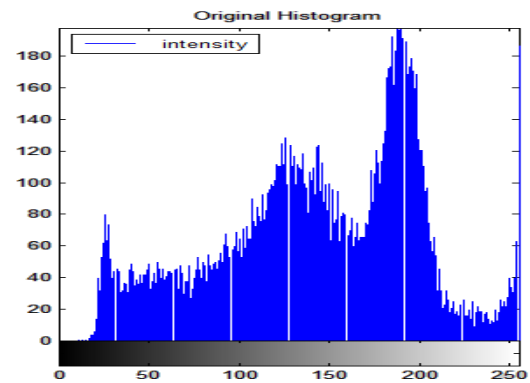
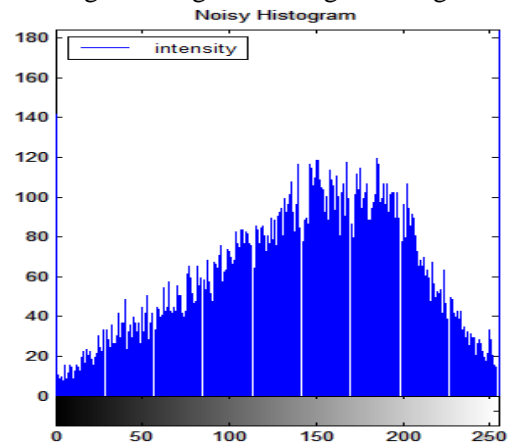
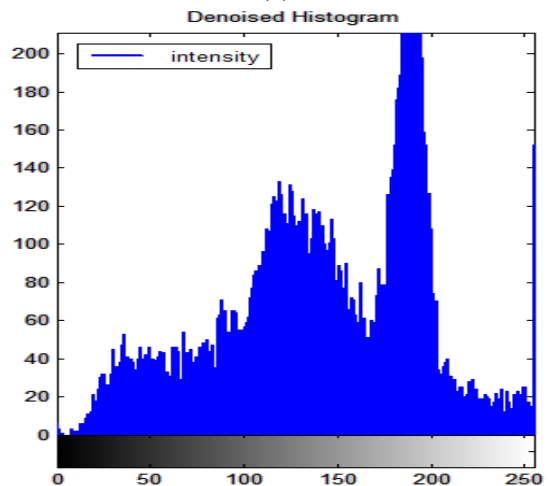


Fig4. Histogram of original image



(a)



(b)

Fig5. Histograms of (a) noisy and (b) denoised images

## V. CONCLUSIONS

In this paper, we presented a modified Discrete Curvelet Transform (M-DCVT) model for texture enhanced image denoising. A simple but theoretically



solid model and the associated algorithm were presented and achieves promising results in enhancing the texture structure while removing random noise. The experimental results demonstrated the effectiveness of proposed MDCVT in texture enhanced image denoising. Most of the state-of-the-art denoising algorithms are based on the local sparsity and nonlocal self-similarity priors of natural images.

## REFERENCES

1. Buades, A, Coll, B, Morel J.M, "A non-local algorithm for image denoising", IEEE Computer Society Conference on Computer Vision and Pattern Recognition, 20-26 June 2005, San Diego, CA, USA.
2. C. Deledalle, V. Duval, and J. Salmon, "Non-local methods with shape adaptive patches (nlm-sap)," *J. Math. Imag. Vis.*, vol. 43, no. 2, pp. 103–120, 2012.
3. V. Duval, J. Aujol, and Y. Gousseau, "A bias-variance approach for the nonlocal means," *SIAM J. Imag. Sci.*, vol. 4, no. 2, pp. 760–788, 2011.
4. D. Van De Ville and M. Kocher, "Sure-based non-local means," *IEEE Signal Process. Lett.*, vol. 16, no. 11, pp. 973–976, Nov. 2009.
5. J. Salmon, "On two parameters for denoising with non-local means," *IEEE Signal Process. Lett.*, vol. 17, no. 3, pp. 269–272, Mar. 2010.
6. J. Darbon, A. Cunha, T. Chan, S. Osher, and G. Jensen, "Fast nonlocal filtering applied to electron cryomicroscopy," in *IEEE Int. Symp. Biomedical Imaging: From Nano to Macro*, 2008, pp. 1331–1334.
7. R. Lai and Y. Yang, "Accelerating non-local means algorithm with random projection," *Electron. Lett.*, vol. 47, no. 3, pp. 182–183, 2011,3.
8. K. Chaudhury, "Acceleration of the shiftbleo(1) algorithm for bilateral filtering and non-local means," *IEEE Trans. Image Process.*, vol. PP, no. 99, 2012, p. 1
9. G. Oppenheim J. M. Poggi M. Misiti, Y. Misiti. Wavelet Toolbox. The MathWorks, Inc.,Natick, Massachusetts 01760, April 2001
10. R. Fergus, B. Singh, A. Hertzmann, S. Roweis, and W. T. Freeman, "Removing camera shake from a single photograph," in Proc. ACMSIGGRAPH, pp. 787-794, 2006.
11. A. Levin, R. Fergus, F. Durand, and W. T. Freeman, "Image and depth from a conventional camera with a coded aperture," in Proc. ACMSIGGRAPH, 2007.
12. D. Krishnan, R. Fergus, "Fast image deconvolution using hyperLaplacian priors," in Proc. Neural Inf. Process. Syst., pp. 1033-1041, 2009.
13. L. Rudin, S. Osher, and E. Fatemi, "Nonlinear total variation based noise removal algorithms," *Physica D*, vol. 60, no. 1-4, pp. 259-268, Nov. 1992.
14. M. Wainwright and S. Simoncelli, "Scale mixtures of gaussians and the statistics of natural images," in Proc. Neural Inf. Process. Syst., vol. 12, pp. 855-861, 1999.
15. J. Portilla, V. Strela, M. J. Wainwright, and E. P. Simoncelli, "Image denoising using a scale mixture of Gaussians in the wavelet domain," *IEEE Trans. Image Process.*, vol. 12, no. 11, pp. 1338-1351, Nov. 2003.
16. M. Elad and M. Aharon, "Image denoising via sparse and redundant representations over learned dictionaries," *IEEE Trans. Image Process.*, vol. 15, no. 12, pp. 3736-3745, Dec. 2006.
17. W. Dong, L. Zhang, G. Shi, and X. Wu, "Image deblurring and superresolution by adaptive sparse domain selection and adaptive regularization," *IEEE Trans. Image Process.*, vol. 20, no. 7, pp. 1838-1857, Jul. 2011.
18. A. Buades, B. Coll, and J. Morel, "A review of image denoising methods, with a new one," *Multiscale Model. Simul.*, vol. 4, no. 2, pp. 490-530, 2005.

19. K. Dabov, A. Foi, V. Katkovnik, and K. Egiazarian, "Image denoising by sparse 3-D transform-domain collaborative filtering," *IEEE Trans. Image Process.*, vol. 16, no. 8, pp. 2080-2095, Aug. 2007.
20. V. Katkovnik, A. Foi, K. Egiazarian, and J. Astola, "From local kernel to nonlocal multiple-model image denoising," *Int. J. Computer Vision*, vol. 86, no. 1, pp. 1-32, Jan. 2010.
21. J. Mairal, F. Bach, J. Ponce, G. Sapiro, and A. Zisserman, "Non-local sparse models for image restoration," in *Proc. Int. Conf. Comput. Vis.*, pp. 2272-2279, Sept. 29 2009-Oct. 2 2009.
22. W. Dong, L. Zhang, and G. Shi, "Centralized sparse representation for image restoration," in *Proc. Int. Conf. Comput. Vis.*, pp. 1259-1266, 6-13 Nov. 2011.
23. W. Dong, L. Zhang, G. Shi, and X. Li, "Nonlocally centralized sparse representation for image restoration," *IEEE Trans. Image Process.*, vol. 22, no. 4, pp. 1620-1630, Apr. 2013.
24. E. Hadjidemetriou, M. D. Grossberg, and S. K. Nayar, "Multiresolution histograms and their use for recognition," *IEEE Trans. Pattern Anal. Mach. Intell.*, vol. 26, no. 7, pp. 831-847, Jul. 2004.
25. M. Varma and A. Zisserman, "A statistical approach to texture classification from single images," *Int. J. Computer Vision*, vol. 62, no. 1-2, pp. 61-81, Apr. 2005.
26. M. Varma and A. Zisserman, "Classifying images of materials: achieving viewpoint and illumination independence," in *Proc. Eur. Conf. Comput. Vis.*, pp. 255-271, 2002.
27. W. Zuo, L. Zhang, C. Song, and D. Zhang, "Texture Enhanced Image Denoising via Gradient Histogram Preservation," in *Proc. Int. Conf. Comput. Vis. Pattern Recognit.*, 2013.